

# Research Journal of Pharmaceutical, Biological and Chemical Sciences

## Physical-Chemical Investigations of Clay Minerals of The Alekseyevskoye Field in The Republic of Kazakhstan.

Aigerim A. Karaubayeva<sup>1\*</sup>, Roza A. Omarova<sup>1</sup>, Zurriyada B. Sakipova<sup>1</sup>,  
Liliya N. Ibragimova<sup>1</sup>, Asyl A. Espenbetov<sup>2</sup>, G. S. Ibadullaeva<sup>1</sup>,  
Evgenyi V. Gladukh<sup>3</sup>, and A. A. Turgumbayeva<sup>1</sup>

<sup>1</sup>Asfendiyarov Kazakh National Medical University, department of pharmaceutical technology, Almaty, the Republic of Kazakhstan

<sup>2</sup>Al-Faraby Kazakh National University, department of inorganic chemistry, the Republic of Kazakhstan

<sup>3</sup>National Pharmaceutical University, department of industrial pharmacy, Kharkov, Ukraine

### ABSTRACT

The data about the element, X-ray diffraction, and infrared-spectroscopic analyses of the kaolinite mineral of the Alekseyevskoye Field, the Republic of Kazakhstan are presented. This data was obtained based on the innovative technology for removal of impurities. It was revealed that due to the applied method of impurities removal from kaolinite the content of clean kaolinite was over 90 % which allows using the obtained kaolin as pharmaceutical substances - excipients and its standardization. Outcomes received from investigation of various-degree phases of impurities removal can be used to identify the composition of cleaned kaolinite, kaolinite with impurities, and native kaolinite. Investigation object is the rock-forming mineral – kaolinite of the Alekseyevskoye Field.

**Keywords:** mineral clay, kaolinite, X-ray diffraction, Infrared-Spectroscopic

*\*Corresponding author*

## INTRODUCTION

Kaolin is widely used in the pharmaceutical, cosmetic, veterinary, and other industries. Therefore when such complexes are studied various investigation methods, including physical-chemical, should be applied to detect their characterizing properties. Suitability of clay minerals use in the medical and pharmaceutical industries is studied under the broad program where HAF and infrared-spectroscopic investigations are the key methods of mineral composition identification.

Kaolin is a clay mineral the clay part of which is represented mainly by kaolinite and rarely by other minerals of the similarly-named group and similar composition that formed as a result of exogenous and hydrothermalkaolinization of aluminum silicates. Also kaolin is the clay mainly consisting of clean kaolinite or related clay minerals with the similar compositions, in its natural state it is white, it can be enriched and refined. There are primary and secondary kaolins depending on the conditions of their occurrence. Primary kaolins occur in the place of parent rock from which they are formed and usually contain up to 50% of mechanically separated impurities – mica, feldspar, quartz, etc., which can be removed by various ways.

The present study was designed to determinate physical and chemical characteristics of the Kaolinite of Alexeyevskoye field.

## MATERIAL AND MEDHODS

For the analysis there was used the DRON-3M X-ray device with the digital data recording attachment; filtered  $\text{CuK}\alpha$ -radiation (copper X-ray target).

X-ray diffraction patterns were recorded under the following conditions:

- wave length - 1.54051 (Å);
- number of points for smoothing ranged from 7 to 9 depending on a sample;
- degree of polynomial background - 3;
- piece-wise approximation of the background - +;
- threshold – 3.0 sigma;
- peak width at base – 3.0 FWHM.

Initial data: FWHM, deg. – 0.160; asymmetry – 1.00; form factor – 0.60.

For the analysis there was used Infra-Red spectra were recorded on a Fourier transform infrared spectrometer Nicolet 6700 (Thermo scientific company, USA) on the console SmurtPerformer with ZnSe crystal by internal reflection.

## RESULTS AND METHODS

### Results from the X-ray Diffraction Analysis of Various Purity Kaolin Samples

It is known that any crystalline matter has its lattice, specific chemical composition, and particular distribution of the atoms in a unit cell of the lattice. A number of interplanar spacing and Bragg angles  $\Theta$  as a result of diffraction in the defined emission can be found in the lattice geometry, as well as types and distributions of the atoms are characterized by the intensity of diffracted beams.<sup>1</sup> Therefore, the X-ray diffraction analysis was performed on the basis of related interplanar spacing (d) and relative line intensities (I) of the X-ray spectrum to identify various crystalline phases found in the various purity kaolin samples of the Alexeyevskoye Field. Four kaolin samples were taken for investigation. X-ray diffraction patterns of the investigated samples are shown in Figures 1-8 and results of the obtained data interpretation are represented in Tables 1-8.

Electronic database of powder diffraction (ICSD) was used for proper interpretation of the X-ray diffraction analysis results. Phase analysis was conducted through comparison of experimental values of interplanar spacing and relative line intensities represented in Tables 1-8 with the standard X-ray diffraction patterns. In tables there were found substances with the most intense lines similar to the data obtained from

experiments. Only the lines with differences between their table and empirical values not exceeding  $\pm 0.02 \text{ \AA}$  within the range of interplanar spacing over  $1.5 \text{ \AA}$  and not exceeding  $\pm 0.01 \text{ \AA}$  within the range of at least  $1.5 \text{ \AA}$  were taken into account.

1

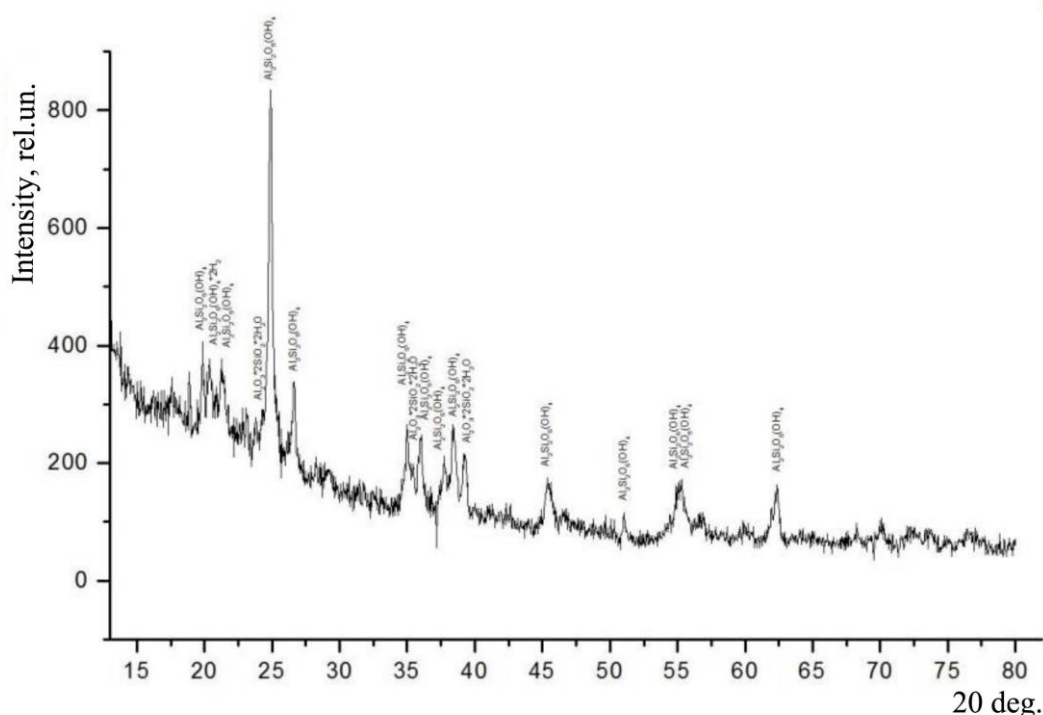


Figure 1 – X-ray diffraction pattern of kaolin sample No. 1

Table 1 – Results from the X-ray diffraction analysis of kaolin sample No.1

2Tmax	lmax	d	2Tcg	lint	w	k	a	R	Phase composition
19.8452	73.6	4.4700	19.8493	1153.2	0.183	0.600	1.000	0.497	Al <sub>2</sub> Si <sub>2</sub> O <sub>5</sub> (OH) <sub>4</sub>
20.3691	56.7	4.3562	20.3850	986.4	0.202	0.600	1.117	0.497	Al <sub>2</sub> Si <sub>2</sub> O <sub>5</sub> (OH) <sub>4</sub> *2H <sub>2</sub> O
21.1955	51.1	4.1882	21.3265	1368.9	0.353	0.600	0.243	0.497	Al <sub>2</sub> Si <sub>2</sub> O <sub>5</sub> (OH) <sub>4</sub>
24.5839	81.5	3.6180	24.6752	1875.3	0.242	0.600	0.610	0.497	Al <sub>2</sub> O <sub>3</sub> *2SiO <sub>2</sub> *2H <sub>2</sub> O
24.8454	392.8	3.5805	24.9165	8757.0	0.234	0.600	0.610	0.497	Al <sub>2</sub> Si <sub>2</sub> O <sub>5</sub> (OH) <sub>4</sub>
26.6807	98.9	3.3383	26.6331	1726.2	0.232	0.600	4.513	0.497	Al <sub>2</sub> Si <sub>2</sub> O <sub>5</sub> (OH) <sub>4</sub>
35.0194	79.0	2.5601	34.9969	1114.6	0.146	0.600	2.092	0.497	Al <sub>2</sub> Si <sub>2</sub> O <sub>5</sub> (OH) <sub>4</sub>
35.7558	68.1	2.5091	35.8518	785.0	0.123	0.600	0.306	0.497	Al <sub>2</sub> O <sub>3</sub> *2SiO <sub>2</sub> *2H <sub>2</sub> O
35.9377	86.9	2.4968	36.0207	1090.1	0.140	0.600	0.306	0.497	Al <sub>2</sub> Si <sub>2</sub> O <sub>5</sub> (OH) <sub>4</sub>
37.7107	43.3	2.3834	37.7912	1048.8	0.271	0.600	0.974	0.497	Al <sub>2</sub> Si <sub>2</sub> O <sub>5</sub> (OH) <sub>4</sub>
38.3409	81.5	2.3456	38.3614	1599.3	0.206	0.600	0.974	0.497	Al <sub>2</sub> Si <sub>2</sub> O <sub>5</sub> (OH) <sub>4</sub>
39.1918	61.1	2.2966	39.2783	1360.8	0.269	0.600	0.531	0.497	Al <sub>2</sub> O <sub>3</sub> *2SiO <sub>2</sub> *2H <sub>2</sub> O
45.3240	42.3	1.9991	45.4931	1754.2	0.582	0.600	0.415	0.497	Al <sub>2</sub> Si <sub>2</sub> O <sub>5</sub> (OH) <sub>4</sub>
51.0234	28.3	1.7884	51.0703	412.1	0.160	0.600	1.000	0.497	Al <sub>2</sub> Si <sub>2</sub> O <sub>5</sub> (OH) <sub>4</sub>
54.8650	37.9	1.6719	54.9280	332.9	0.090	0.600	1.000	0.497	Al <sub>2</sub> Si <sub>2</sub> O <sub>5</sub> (OH) <sub>4</sub> *2H <sub>2</sub> O
55.1746	45.9	1.6633	55.2428	2307.8	0.607	0.600	1.000	0.497	Al <sub>2</sub> Si <sub>2</sub> O <sub>5</sub> (OH) <sub>4</sub>
62.3383	62.6	1.4882	62.2714	2195.6	0.418	0.600	2.800	0.497	Al <sub>2</sub> Si <sub>2</sub> O <sub>5</sub> (OH) <sub>4</sub>

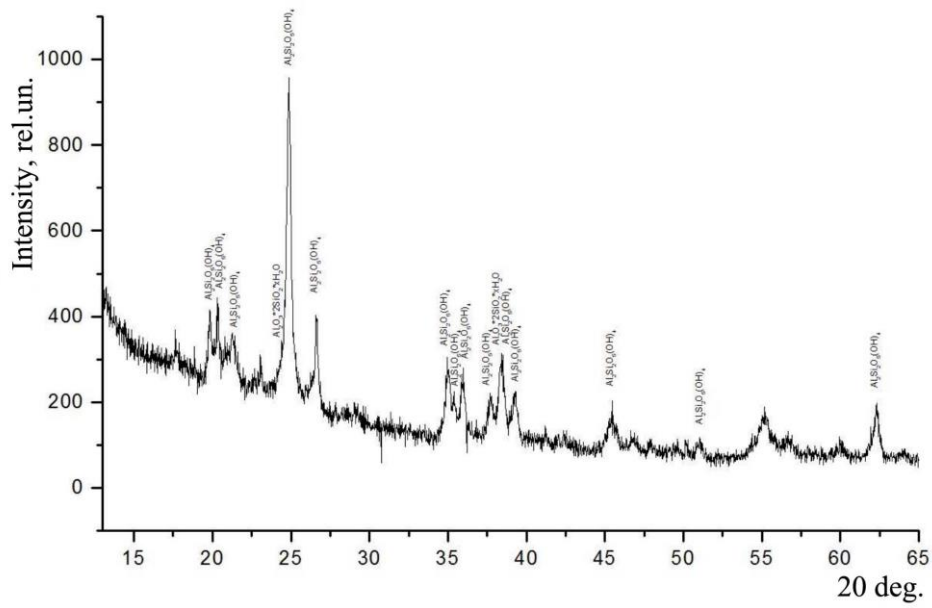


Figure 2 – X-ray diffraction pattern of kaolin sample No. 2

Table 2 – Results from the X-ray diffraction analysis of kaolin sample No.2

2Tmax	lmax	d	2Tcg	lint	w	k	a	R	Phase composition
19.8452	96.4	4.4700	19.8684	1823.1	0.217	0.600	1.453	0.497	Al <sub>2</sub> Si <sub>2</sub> O <sub>5</sub> (OH) <sub>4</sub>
20.3382	92.5	4.3627	20.3036	2312.7	0.271	0.600	1.453	0.497	Al <sub>2</sub> Si <sub>2</sub> O <sub>5</sub> (OH) <sub>4</sub>
21.2567	55.3	4.1762	21.3278	1668.5	0.406	0.600	0.609	0.497	Al <sub>2</sub> Si <sub>2</sub> O <sub>5</sub> (OH) <sub>4</sub>
24.6924	215.1	3.6024	24.7066	3304.5	0.160	0.600	1.000	0.497	Al <sub>2</sub> O <sub>3</sub> *2SiO <sub>2</sub> *xH <sub>2</sub> O
24.8640	550.2	3.5779	24.8657	8317.9	0.160	0.600	1.000	0.497	Al <sub>2</sub> Si <sub>2</sub> O <sub>5</sub> (OH) <sub>4</sub>
26.5943	149.0	3.3489	26.6341	2447.7	0.188	0.600	0.766	0.497	Al <sub>2</sub> Si <sub>2</sub> O <sub>5</sub> (OH) <sub>4</sub>
34.9636	99.9	2.5641	34.9601	2639.6	0.282	0.600	1.635	0.497	Al <sub>2</sub> Si <sub>2</sub> O <sub>5</sub> (OH) <sub>4</sub>
35.3931	53.4	2.5339	35.3671	1175.4	0.226	0.600	1.635	0.497	Al <sub>2</sub> Si <sub>2</sub> O <sub>5</sub> (OH) <sub>4</sub>
35.9497	92.5	2.4960	35.8728	2737.8	0.312	0.600	1.635	0.497	Al <sub>2</sub> Si <sub>2</sub> O <sub>5</sub> (OH) <sub>4</sub>
37.6660	50.6	2.3861	37.7347	1535.1	0.402	0.600	0.602	0.497	Al <sub>2</sub> Si <sub>2</sub> O <sub>5</sub> (OH) <sub>4</sub>
38.2871	82.8	2.3488	38.3350	1385.6	0.181	0.600	1.253	0.497	Al <sub>2</sub> O <sub>3</sub> *2SiO <sub>2</sub> *xH <sub>2</sub> O
38.4838	90.7	2.3372	38.5181	2119.0	0.250	0.600	1.253	0.497	Al <sub>2</sub> Si <sub>2</sub> O <sub>5</sub> (OH) <sub>4</sub>
39.2418	59.9	2.2938	39.1977	1834.3	0.339	0.600	1.253	0.497	Al <sub>2</sub> Si <sub>2</sub> O <sub>5</sub> (OH) <sub>4</sub>
45.3737	42.0	1.9971	45.4506	1898.6	0.567	0.600	0.866	0.497	Al <sub>2</sub> Si <sub>2</sub> O <sub>5</sub> (OH) <sub>4</sub>
51.0112	27.5	1.7888	51.0403	527.0	0.227	0.600	1.448	0.497	Al <sub>2</sub> Si <sub>2</sub> O <sub>5</sub> (OH) <sub>4</sub>
62.2845	82.7	1.4894	62.2952	1973.9	0.264	0.600	1.723	0.497	Al <sub>2</sub> Si <sub>2</sub> O <sub>5</sub> (OH) <sub>4</sub>

Sample 3, Layer 1

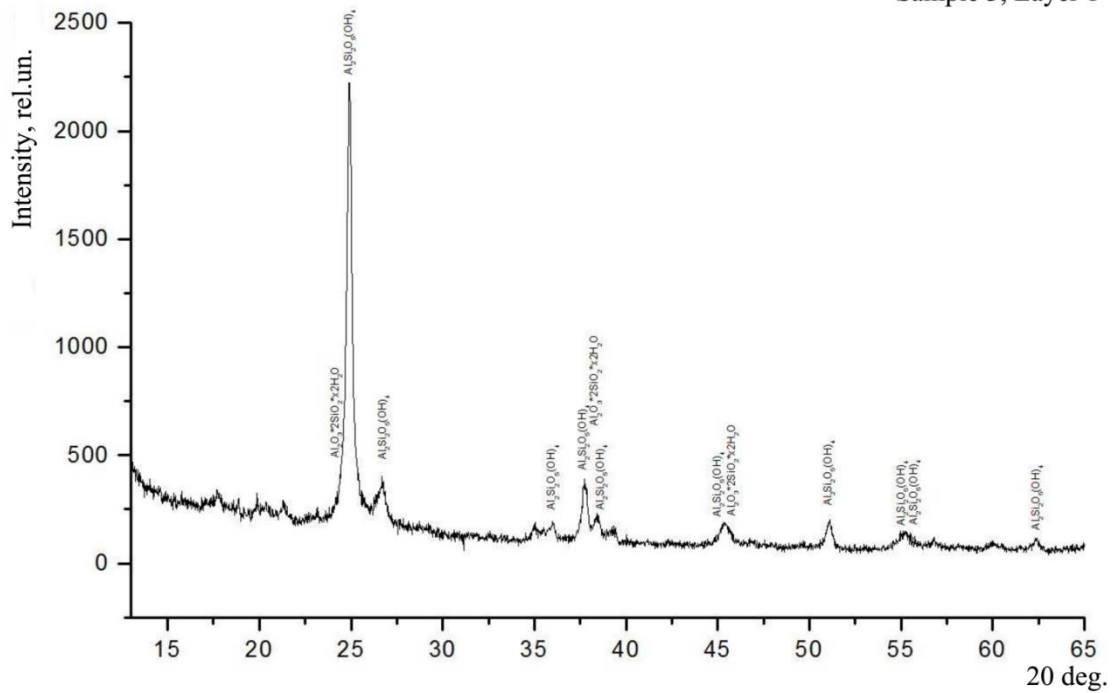


Figure 3 – X-ray diffraction pattern of kaolin sample No. 3, layer 1

Table 3 – Results from the X-ray diffraction analysis of kaolin sample No.3, layer 1

2Tmax	lmax	d	2Tcg	lint	w	k	a	R	Phase composition
24.7421	618.7	3.5953	24.7823	9848.9	0.160	0.600	1.000	0.497	Al <sub>2</sub> O <sub>3</sub> *2SiO <sub>2</sub> *x2H <sub>2</sub> O
24.9124	1574.8	3.5711	24.9479	25150.0	0.160	0.600	1.000	0.497	Al <sub>2</sub> Si <sub>2</sub> O <sub>5</sub> (OH) <sub>4</sub>
26.5888	171.7	3.3496	26.5834	2710.8	0.160	0.600	1.000	0.497	Al <sub>2</sub> Si <sub>2</sub> O <sub>5</sub> (OH) <sub>4</sub>
36.0281	42.0	2.4907	35.9924	839.7	0.257	0.600	3.237	0.497	Al <sub>2</sub> Si <sub>2</sub> O <sub>5</sub> (OH) <sub>4</sub>
37.7123	217.9	2.3833	37.7644	3441.0	0.160	0.600	1.000	0.497	Al <sub>2</sub> Si <sub>2</sub> O <sub>5</sub> (OH) <sub>4</sub>
37.9006	59.4	2.3719	37.9463	942.5	0.160	0.600	1.000	0.497	Al <sub>2</sub> O <sub>3</sub> *2SiO <sub>2</sub> *x2H <sub>2</sub> O
38.3778	100.0	2.3435	38.4099	1593.3	0.160	0.600	1.000	0.497	Al <sub>2</sub> Si <sub>2</sub> O <sub>5</sub> (OH) <sub>4</sub>
45.0545	38.9	2.0105	45.2083	834.0	0.230	0.600	0.389	0.497	Al <sub>2</sub> O <sub>3</sub> *2SiO <sub>2</sub> *x2H <sub>2</sub> O
45.4193	50.5	1.9952	45.5599	1566.8	0.355	0.600	0.389	0.497	Al <sub>2</sub> Si <sub>2</sub> O <sub>5</sub> (OH) <sub>4</sub>
50.9725	40.0	1.7901	51.0196	995.9	0.279	0.600	1.185	0.497	Al <sub>2</sub> Si <sub>2</sub> O <sub>5</sub> (OH) <sub>4</sub>
54.9541	35.9	1.6694	55.0392	530.9	0.160	0.600	0.798	0.497	Al <sub>2</sub> Si <sub>2</sub> O <sub>5</sub> (OH) <sub>4</sub>
55.2252	32.8	1.6619	55.2852	800.5	0.278	0.600	0.798	0.497	Al <sub>2</sub> Si <sub>2</sub> O <sub>5</sub> (OH) <sub>4</sub>
62.3836	34.6	1.4873	62.3860	594.3	0.203	0.600	2.750	0.497	Al <sub>2</sub> Si <sub>2</sub> O <sub>5</sub> (OH) <sub>4</sub>

Sample 3, Layer 2

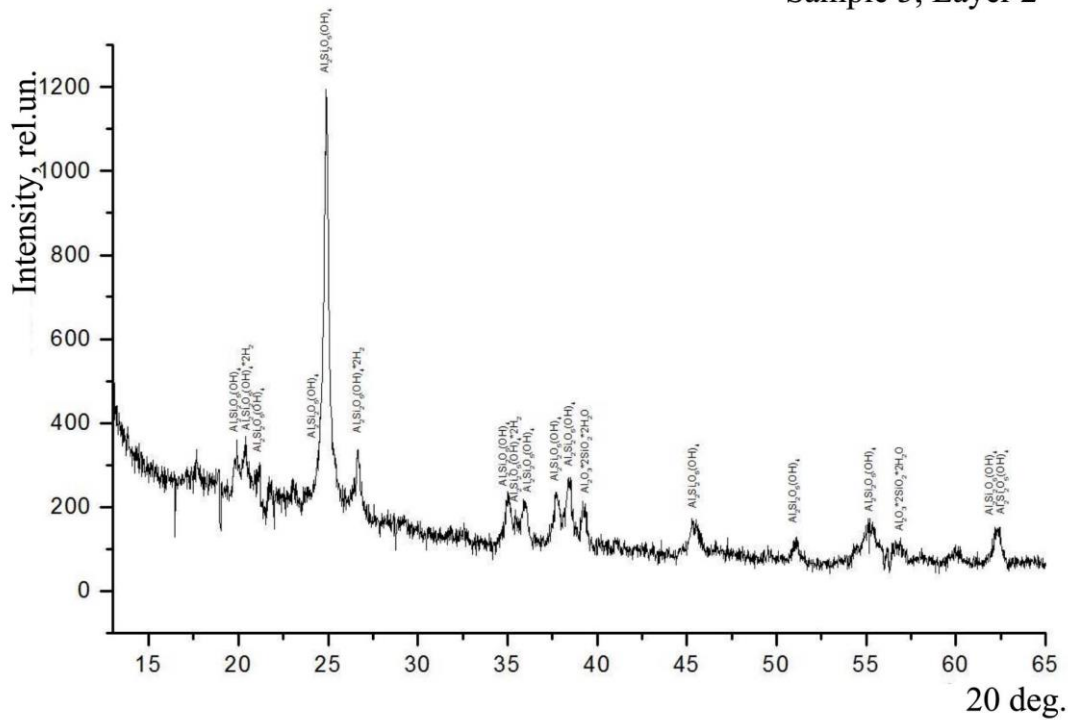


Figure 4 – X-ray diffraction pattern of kaolin sample No. 3, layer 2

Table 4 – Results from the X-ray diffraction analysis of kaolin sample No.3, layer 2

2Tmax	lmax	d	2Tcg	lint	w	k	a	R	Phase composition
19.9113	58.2	4.4553	19.8673	1396.0	0.272	0.600	2.304	0.497	Al <sub>2</sub> Si <sub>2</sub> O <sub>5</sub> (OH) <sub>4</sub>
20.3867	60.5	4.3524	20.2773	1765.7	0.323	0.600	2.304	0.497	Al <sub>2</sub> Si <sub>2</sub> O <sub>5</sub> (OH) <sub>4</sub> *2H <sub>2</sub> O
21.1902	58.4	4.1892	21.1125	716.3	0.140	0.600	12.551	0.497	Al <sub>2</sub> Si <sub>2</sub> O <sub>5</sub> (OH) <sub>4</sub>
24.6446	137.2	3.6093	24.6798	3170.3	0.242	0.600	1.043	0.497	Al <sub>2</sub> Si <sub>2</sub> O <sub>5</sub> (OH) <sub>4</sub>
24.8837	608.8	3.5751	24.9030	12447.2	0.211	0.600	1.043	0.497	Al <sub>2</sub> Si <sub>2</sub> O <sub>5</sub> (OH) <sub>4</sub>
26.6749	86.9	3.3390	26.6480	2775.4	0.376	0.600	1.602	0.497	Al <sub>2</sub> Si <sub>2</sub> O <sub>5</sub> (OH) <sub>4</sub> *2H <sub>2</sub> O
35.0319	76.4	2.5592	35.1054	2038.0	0.335	0.600	1.382	0.497	Al <sub>2</sub> Si <sub>2</sub> O <sub>5</sub> (OH) <sub>4</sub>
35.4612	35.8	2.5292	35.4699	585.5	0.168	0.600	1.382	0.497	Al <sub>2</sub> Si <sub>2</sub> O <sub>5</sub> (OH) <sub>4</sub> *2H <sub>2</sub> O
35.8423	41.9	2.5032	35.8196	977.6	0.245	0.600	1.382	0.497	Al <sub>2</sub> Si <sub>2</sub> O <sub>5</sub> (OH) <sub>4</sub>
37.7252	72.7	2.3825	37.7890	2141.3	0.316	0.600	1.108	0.497	Al <sub>2</sub> Si <sub>2</sub> O <sub>5</sub> (OH) <sub>4</sub>
38.4066	97.6	2.3418	38.4201	3206.0	0.343	0.600	1.108	0.497	Al <sub>2</sub> Si <sub>2</sub> O <sub>5</sub> (OH) <sub>4</sub>
39.2355	55.4	2.2942	39.1860	1396.5	0.280	0.600	1.108	0.497	Al <sub>2</sub> O <sub>3</sub> *2SiO <sub>2</sub> *2H <sub>2</sub> O
45.5558	37.4	1.9895	45.5634	1299.7	0.397	0.600	1.143	0.497	Al <sub>2</sub> Si <sub>2</sub> O <sub>5</sub> (OH) <sub>4</sub>
50.9403	37.4	1.7911	51.1269	898.5	0.276	0.600	0.191	0.497	Al <sub>2</sub> Si <sub>2</sub> O <sub>5</sub> (OH) <sub>4</sub>
55.2312	46.9	1.6617	55.1442	3513.4	0.984	0.600	1.538	0.497	Al <sub>2</sub> Si <sub>2</sub> O <sub>5</sub> (OH) <sub>4</sub>
56.7589	26.4	1.6205	56.7716	777.7	0.336	0.600	1.000	0.497	Al <sub>2</sub> O <sub>3</sub> *2SiO <sub>2</sub> *2H <sub>2</sub> O
62.2228	35.5	1.4907	62.2472	653.7	0.208	0.600	1.982	0.497	Al <sub>2</sub> Si <sub>2</sub> O <sub>5</sub> (OH) <sub>4</sub>
62.4013	37.5	1.4869	62.3972	868.1	0.258	0.600	1.982	0.497	Al <sub>2</sub> Si <sub>2</sub> O <sub>5</sub> (OH) <sub>4</sub>



Sample 4, Layer 1

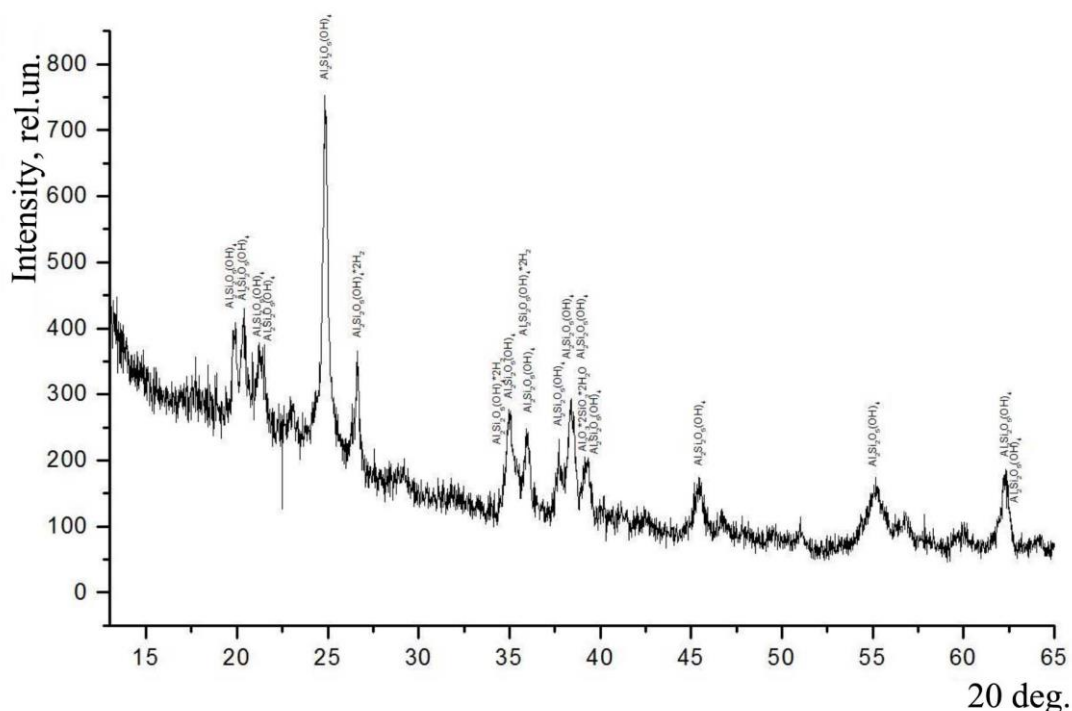


Figure 6 – X-ray diffraction pattern of kaolin sample No. 4, layer 1

Table 6 – Results from the X-ray diffraction analysis of kaolin sample No.4, layer 1

2Tmax	lmax	d	2Tcg	lint	w	k	a	R	Phase composition
19.7683	87.7	4.4872	19.9865	2321.0	0.283	0.600	0.164	0.497	Al <sub>2</sub> Si <sub>2</sub> O <sub>5</sub> (OH) <sub>4</sub>
20.2536	75.3	4.3808	20.4487	2354.6	0.369	0.600	0.164	0.497	Al <sub>2</sub> Si <sub>2</sub> O <sub>5</sub> (OH) <sub>4</sub>
21.1721	74.2	4.1927	21.2090	1092.3	0.160	0.600	1.000	0.497	Al <sub>2</sub> Si <sub>2</sub> O <sub>5</sub> (OH) <sub>4</sub>
21.4069	70.8	4.1473	21.4222	1067.5	0.160	0.600	1.000	0.497	Al <sub>2</sub> Si <sub>2</sub> O <sub>5</sub> (OH) <sub>4</sub>
24.8525	330.2	3.5795	24.8643	8798.4	0.290	0.600	1.103	0.497	Al <sub>2</sub> Si <sub>2</sub> O <sub>5</sub> (OH) <sub>4</sub>
26.6387	96.7	3.3434	26.5939	2031.1	0.238	0.600	2.176	0.497	Al <sub>2</sub> Si <sub>2</sub> O <sub>5</sub> (OH) <sub>4</sub> *2H <sub>2</sub> O
34.6852	63.0	2.5840	34.7081	71.1	0.012	0.600	1.294	0.497	Al <sub>2</sub> O <sub>3</sub> *2SiO <sub>2</sub> *xH <sub>2</sub> O
34.9060	68.2	2.5682	34.9320	1021.2	0.154	0.600	1.294	0.497	Al <sub>2</sub> Si <sub>2</sub> O <sub>5</sub> (OH) <sub>4</sub>
35.2581	42.9	2.5433	35.2550	2688.3	0.736	0.600	1.294	0.497	Al <sub>2</sub> Si <sub>2</sub> O <sub>5</sub> (OH) <sub>4</sub> *2H <sub>2</sub> O
35.9699	73.4	2.4946	35.9194	1954.4	0.286	0.600	1.294	0.497	Al <sub>2</sub> Si <sub>2</sub> O <sub>5</sub> (OH) <sub>4</sub>
37.7089	50.7	2.3835	37.7865	1432.6	0.308	0.600	1.094	0.497	Al <sub>2</sub> Si <sub>2</sub> O <sub>5</sub> (OH) <sub>4</sub>
38.2220	50.5	2.3526	38.2548	1083.5	0.219	0.600	1.094	0.497	Al <sub>2</sub> Si <sub>2</sub> O <sub>5</sub> (OH) <sub>4</sub> *2H <sub>2</sub> O
38.3848	85.4	2.3430	38.4108	1640.7	0.195	0.600	1.094	0.497	Al <sub>2</sub> Si <sub>2</sub> O <sub>5</sub> (OH) <sub>4</sub>
38.5591	62.8	2.3328	38.5802	1032.8	0.166	0.600	1.094	0.497	Al <sub>2</sub> Si <sub>2</sub> O <sub>5</sub> (OH) <sub>4</sub>
39.0598	33.8	2.3041	39.0645	521.8	0.157	0.600	1.094	0.497	Al <sub>2</sub> O <sub>3</sub> *2SiO <sub>2</sub> *2H <sub>2</sub> O
39.2873	48.8	2.2913	39.2551	1177.2	0.260	0.600	1.094	0.497	Al <sub>2</sub> Si <sub>2</sub> O <sub>5</sub> (OH) <sub>4</sub>
45.4537	38.9	1.9937	45.4406	1422.6	0.485	0.600	1.807	0.497	Al <sub>2</sub> Si <sub>2</sub> O <sub>5</sub> (OH) <sub>4</sub>
55.1166	42.8	1.6649	55.0530	3029.7	0.920	0.600	1.232	0.497	Al <sub>2</sub> Si <sub>2</sub> O <sub>5</sub> (OH) <sub>4</sub>
62.2593	58.4	1.4899	62.2154	1768.2	0.346	0.600	2.258	0.497	Al <sub>2</sub> Si <sub>2</sub> O <sub>5</sub> (OH) <sub>4</sub>
62.4261	29.0	1.4863	62.3671	729.2	0.283	0.600	2.258	0.497	Al <sub>2</sub> Si <sub>2</sub> O <sub>5</sub> (OH) <sub>4</sub>

Sample 4, Layer 2

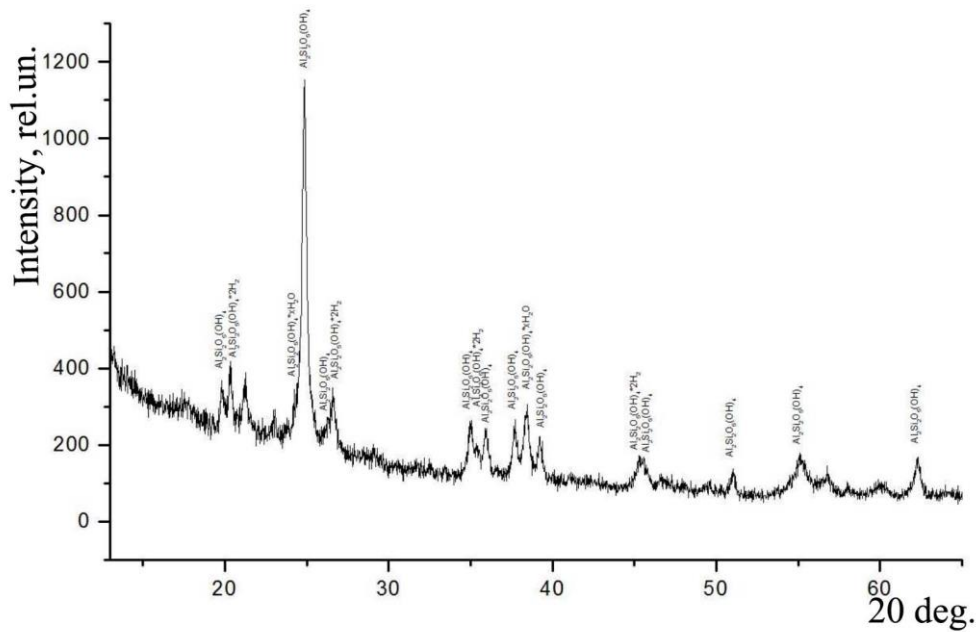


Figure 7 – X-ray diffraction pattern of kaolin sample No. 4, layer 2

Table 7 – Results from the X-ray diffraction analysis of kaolin sample No.4, layer 2

2Tmax	lmax	d	2Tcg	lint	w	k	a	R	Phase composition
19.7880	62.9	4.4828	19.8431	1066.9	0.198	0.600	0.572	0.497	Al <sub>2</sub> Si <sub>2</sub> O <sub>5</sub> (OH) <sub>4</sub>
20.3437	84.6	4.3616	20.3535	1182.3	0.159	0.600	1.288	0.497	Al <sub>2</sub> Si <sub>2</sub> O <sub>5</sub> (OH) <sub>4</sub> *2H <sub>2</sub> O
24.5349	50.6	3.6251	24.6270	1695.2	0.368	0.600	0.815	0.497	Al <sub>2</sub> Si <sub>2</sub> O <sub>5</sub> (OH) <sub>4</sub> *xH <sub>2</sub> O
24.8296	593.5	3.5828	24.8842	16815.1	0.300	0.600	0.815	0.497	Al <sub>2</sub> Si <sub>2</sub> O <sub>5</sub> (OH) <sub>4</sub>
26.2903	46.0	3.3869	26.3340	685.3	0.160	0.600	1.000	0.497	Al <sub>2</sub> Si <sub>2</sub> O <sub>5</sub> (OH) <sub>4</sub>
26.5790	110.3	3.3508	26.6001	1687.2	0.160	0.600	1.000	0.497	Al <sub>2</sub> Si <sub>2</sub> O <sub>5</sub> (OH) <sub>4</sub> *2H <sub>2</sub> O
34.9730	84.9	2.5634	35.0708	2272.5	0.307	0.600	0.998	0.497	Al <sub>2</sub> Si <sub>2</sub> O <sub>5</sub> (OH) <sub>4</sub>
35.3864	34.9	2.5344	35.4351	1041.6	0.317	0.600	0.998	0.497	Al <sub>2</sub> Si <sub>2</sub> O <sub>5</sub> (OH) <sub>4</sub> *2H <sub>2</sub> O
35.9119	74.5	2.4985	35.9200	1926.0	0.273	0.600	0.998	0.497	Al <sub>2</sub> Si <sub>2</sub> O <sub>5</sub> (OH) <sub>4</sub>
37.6539	77.6	2.3868	37.7703	2036.6	0.278	0.600	0.763	0.497	Al <sub>2</sub> Si <sub>2</sub> O <sub>5</sub> (OH) <sub>4</sub>
38.2971	81.7	2.3482	38.3712	2186.5	0.276	0.600	0.763	0.497	Al <sub>2</sub> Si <sub>2</sub> O <sub>5</sub> (OH) <sub>4</sub> *xH <sub>2</sub> O
38.4672	65.7	2.3382	38.5260	1251.7	0.194	0.600	0.763	0.497	Al <sub>2</sub> Si <sub>2</sub> O <sub>5</sub> (OH) <sub>4</sub>
39.0650	35.5	2.3038	39.1010	222.0	0.062	0.600	0.763	0.497	Al <sub>2</sub> O <sub>3</sub> *2SiO <sub>2</sub> *2H <sub>2</sub> O
39.2144	70.5	2.2954	39.2342	1089.5	0.165	0.600	0.763	0.497	H <sub>4</sub> Al <sub>2</sub> Si <sub>2</sub> O <sub>9</sub>
45.2424	37.1	2.0026	45.2886	877.7	0.261	0.600	1.233	0.497	Al <sub>2</sub> Si <sub>2</sub> O <sub>5</sub> (OH) <sub>4</sub> *xH <sub>2</sub> O
45.5551	34.3	1.9895	45.5607	1257.2	0.416	0.600	1.233	0.497	Al <sub>2</sub> Si <sub>2</sub> O <sub>5</sub> (OH) <sub>4</sub>
51.0909	36.7	1.7862	50.9981	815.6	0.266	0.600	7.666	0.497	Al <sub>2</sub> Si <sub>2</sub> O <sub>5</sub> (OH) <sub>4</sub>
55.0698	42.2	1.6662	55.1661	1642.0	0.526	0.600	0.809	0.497	Al <sub>2</sub> Si <sub>2</sub> O <sub>5</sub> (OH) <sub>4</sub>
62.2797	48.5	1.4895	62.3384	1072.8	0.239	0.600	0.923	0.497	Al <sub>2</sub> Si <sub>2</sub> O <sub>5</sub> (OH) <sub>4</sub>



different valencies and this charge is compensated by introduction of such aluminosilicate cations as  $\text{Na}^+$ ,  $\text{K}^+$ ,  $\text{Mg}^{2+}$  to the crystal lattice. This is evidenced by the results (Table 9) which we received based on computation of Sample No.2 X-ray spectrum that implies that the investigated samples contain a certain quantity of the mentioned elements.

**Table 9 – Content of Sample No.2 elements subsequent to the results of X-ray diffraction analysis, %**

Sample No.2 Spectrum	O	Na	Mg	Al	Si	S	Cl	K
	55,60	0,32	0,37	19,01	21,09	0,15	0,45	1,89

According to the authors of this paper <sup>5</sup>, continuous sheets of the silicon oxygen tetrahedrons underlay in the crystal structure of the above-noted fractions. These sheets are weakly linked and this provides sufficiently high cleavage of fractions and different applying of one sheet on the other, which causes some changes in symmetry of the entire crystal lattice. Crystal structure consists of two-sheet packets that contain one oxygen tetrahedral sheet composed of  $[\text{Si}_{2n}\text{O}_{5n}]_{2n}$  and one aluminum-oxygen-hydroxyl octahedral sheet composed of  $[\text{Al}_{2n}(\text{OH})_{4n}]_{2n}$ . Both sheets are linked into a packet via common oxygen of the silicon-oxygen sheet.

Accordingly, following the results of the X-ray diffraction analysis the composition of investigated kaolin samples is mineral which is typical for sedimentary rocks. They are polymineral systems, mainly with the aluminosilicate composition, including quartz, clay minerals, mica, and feldspars.

**Results from the Infrared-Spectroscopic Investigation of Various Purity Kaolin Samples**

Results of the mineral composition of clay samples obtained in the course of investigations through the X-ray diffraction analysis and described above do not give the complete idea about the structure of investigated objects since it is X-ray amorphous. In this connection, the objective of further investigations is to study composition, type, and character of structural bonds in the material using the infrared spectroscopy. The latter is one of the widely used methods in investigating the structural-group composition of materials applied in various areas of human activities and associated with manufacturing of new materials. Individuality of compound spectra, i.e. no identical spectra in two different compounds, makes it possible to perform the sufficiently correct determination of the molecular structure in a material. Thanks to this fact one can clearly interpret structural bonds' types and characters and presence of any molecular groups in a material independently on their features (amorphous, micro- and nanocrystalline, etc.). <sup>1, 2</sup> That is why we performed the infrared-spectroscopic investigation of analyzed kaolin samples to characterize them more completely.

IR spectra were recorded on the Nicolet 6700 Fourier Infrared Spectrophotometer manufactured by Thermo Scientific (USA) on the SmurtPerformer attachment with the ZnSe crystal using the internal reflection method. Spectra images are shown in Figures 9-13. Assignments of main vibrational frequencies are listed in the Table.

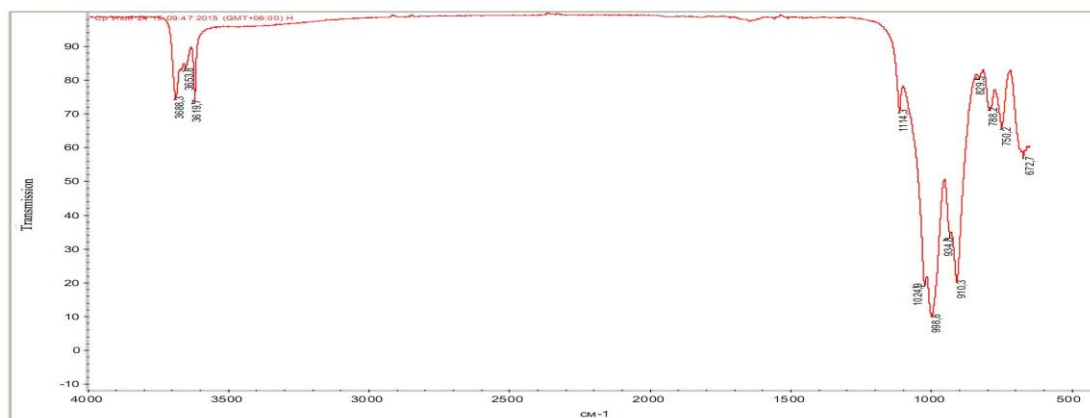


Figure 9 – IR spectrum of sample H

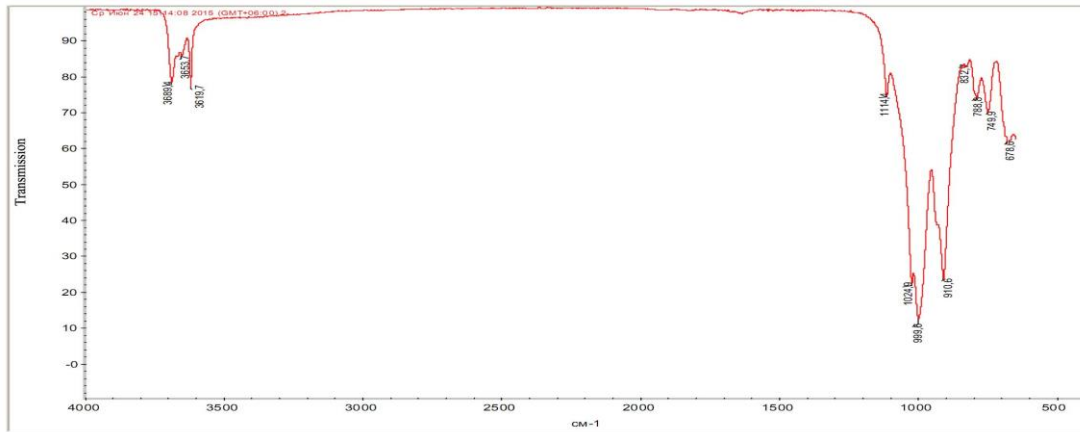


Figure 10 – IR spectrum of sample No.2

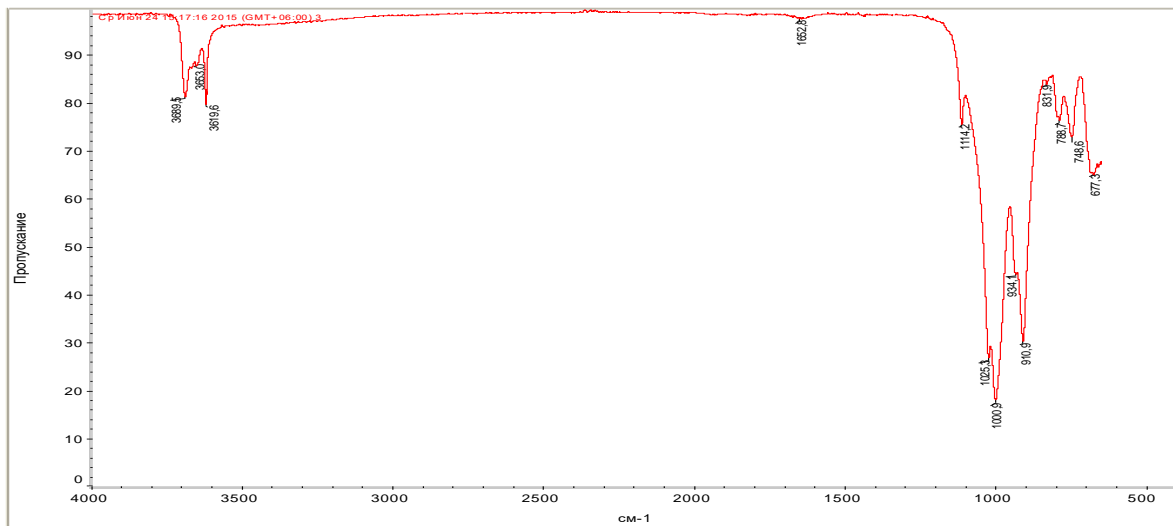


Figure 11 – IR spectrum of sample No.3

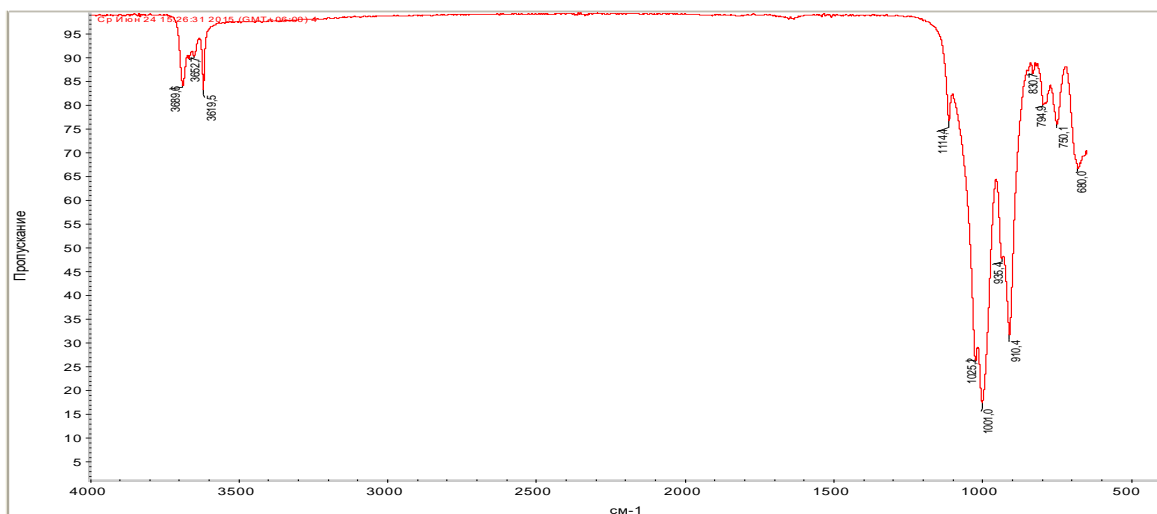


Figure 12 – IR spectrum of sample No.4

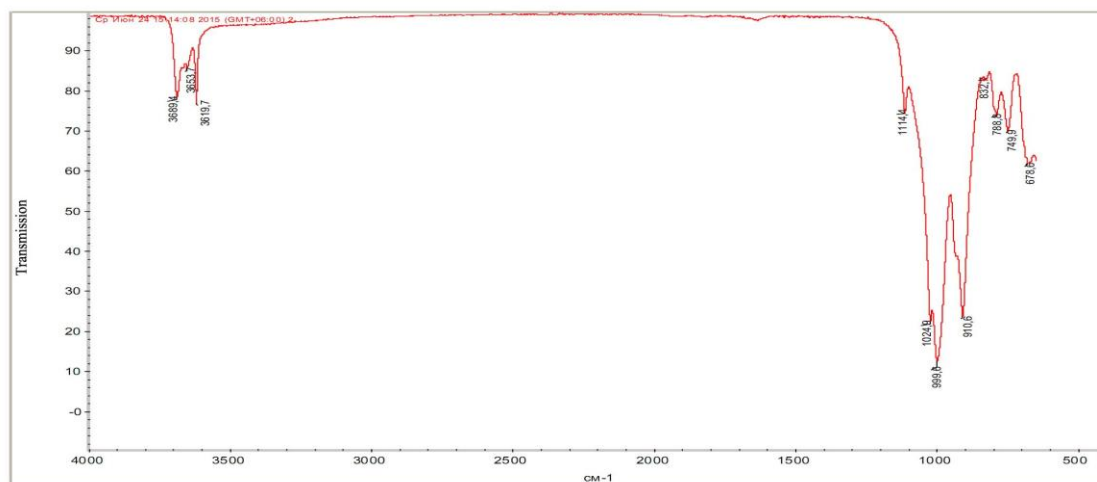


Figure 13 – IR spectrum of sample No. 5

Table 10 – Assignment of vibrational frequencies in the IR spectra of kaolin samples

Assignment	Sample H	Sample No. 2	Sample No. 3	Sample No. 4	Sample No. 5
$\nu^{as}$ (O-H)	3688 m.i. 3654 w.i.	3689 m.i. 3654 w.i.	3690 m.i. 3653 w.i.	3690 m.i. 3652 w.i.	3689 m.i. 3653 w.i.
$\nu^s$ (O-H)	3620 m.i.				
$\nu^{as}$ (Si-O-Si)	1114 m.i.				
$\nu^s$ (Si-O-Si)	1025 s.i.				
$\nu^{as}$ (Si-O)	999 v.s. 935	1000 v.s. -	1001 v.s. 934	1001 v.s. 935 пп.	1001 v.s. 935
$\nu^s$ (Si-O)	910 s.i.	911 s.i.	911 s.i.	910 s.i.	911 s.i.
$\nu^{as}$ (- Si-O-Al)	830 v.w. 778 w.i.	833 v.w. 788 w.i.	832 v.w. 789 сп.	831 v.w. 795 w.i.	829 v.w. 790 w.i.
$\nu^s$ (- Si-O-Al)	750 m.i.	750 m.i.	749 m.i.	750 m.i.	750 m.i.
$\delta$ (Si-O-Si)	673 m.i.	679 m.i.	677 m.i.	680 m.i.	671 m.i.

Notes: m.i. – medium intensity; w.i. – weak intensity; s.i. – strong intensity; v.s. – very strong intensity; v.w. – very weak intensity.

As the Figures and Table shows, there was observed the identical spectral pattern in the spectra of all investigated samples: absorption bands occur at virtually the same frequencies and have almost the same intensity.

In particular, the spectra of all kaolin samples show absorption bands at 3,700-3,600  $\text{cm}^{-1}$  induced by O-H stretching vibrations and this suggests that there are water molecules in their composition. More high-frequency component in this area is typical for antisymmetric stretching modes and more low-frequency component is typical for symmetrical O-H stretching modes. High structuredness and location of these bands in the spectra demonstrates its crystallizing character and confirms the conclusion that had been previously made on the basis of the X-ray diffraction analysis.

There are absorption bands of such groups as Si-O; Si-O-Al; Si-O-Si in all investigated spectra at 1200-600  $\text{cm}^{-1}$ . Location and intensity of the bands is in good agreement with the known literature data.<sup>3, 4</sup> More intense absorption bands in this range (1,000 and 910  $\text{cm}^{-1}$ ) occur due to Si-O- stretching modes and this can be explained by a great number of SiO<sub>2</sub> carcass structure fragments and fields pars in the structure of investigated samples.

Absorption bands at 1,114 and 1,025, 790-778 and 750  $\text{cm}^{-1}$  are linked by stretching modes of Si-O-Si(Al) bridges and this fact says about presence of kaolinoid in the crystal lattice of investigated samples. This is

coherent with layered structure of the latter the anion of which can be described by the  $Q^3$  structural group [5].

Bands at  $680-671\text{ cm}^{-1}$  belong to Si–O–Si bending vibrations, including the bridge oxygen. <sup>6</sup>

H-O-H bending vibrations (in water molecule) make some contribution to vibrations at  $1,200-900\text{ cm}^{-1}$  which leads to occurrence of bends (shoulders) in some main bands and this is explained by their stretching and bending character.

Therefore, results of the infrared-spectroscopic investigation of kaolin samples verify the results of their phase composition determined on the basis of the X-ray diffraction analysis.

### CONCLUSIONS

In the course of investigations there were undertaken full-scale studies of clay minerals for the purpose of their use in medical practices, pharmacies, and health care.

### REFERENCES

- [1] Kovba L.M. X-ray analysis. - MNU. Moscow: 1976. P. 232
- [2] Knyazev A.B., Suleimanov E.V. Basics of X-ray diffraction: Training Toolkit. Nizhny-Novgorod National University of name Lobachevsky, 2005.-P. 232.
- [3] A report on the research work on the topic: «The development of composites of local raw materials for the production of sanitary ceramics, porcelain and tiles». Number of national registration #0112PK00967. Kazakhstan. Almaty 2012. – P 46.
- [4] Vaklova T.V., Habas T.A., Vereshagin V.I. Clay. Structural features and methods.- Tomsk, 2005. – P.248.
- [5] Pashenko A.A., Myasnikov A.A. Physical Chemistry of silicates. High school. Moscow. 1986. – P.368
- [6] Ivashkevich L.S., Karatayeva T.P. Lyahov A.S. X-ray diffraction methods in chemical investigation. Minsk, 2001. P. 227.